

Circumstantial evidence for hydrogen-induced surface magnetism on Pd(110)

P. Amann,^{1,*} M. Cordin,¹ J. Redinger,² S. D. Stolwijk,³ K. Zumbrägel,³ M. Donath,³ E. Bertel,¹ and A. Menzel¹

¹*Institute of Physical Chemistry, University of Innsbruck, Innrain 52a, 6020 Innsbruck, Austria*

²*Institute of Applied Physics, Vienna University of Technology, Gusshausstrasse 25/134, 1040 Vienna, Austria*

³*Physikalisches Institut, Westfälische Wilhelms-Universität Münster, Wilhelm-Klemm-Strasse 10, 48149 Münster, Germany*

(Received 24 November 2011; published 27 March 2012; corrected 6 April 2012)

The surface of clean and hydrogen-covered Pd(110) was investigated by angle-resolved photoemission spectroscopy. At a coverage of 1.5 ML, where the surface adapts a pairing-row reconstruction, the spectra show a peculiar peak splitting of the \bar{S} -surface resonance. The band dispersion of this satellite is parallel to the dispersion of the main resonance but shifted by 400 meV at $T = 100$ K. An interpretation in terms of magnetic exchange splitting is supported by the appearance of a kink structure of the photoemission data around 350 meV binding energy. This unexpected behavior for H adsorption is attributed to the reduced coordination of the Pd atoms at the surface.

DOI: [10.1103/PhysRevB.85.094428](https://doi.org/10.1103/PhysRevB.85.094428)

PACS number(s): 73.20.-r, 79.60.-i

Although all transition metals provide narrow d bands and a high density of states (DOS) at the Fermi level, which favors magnetism, only three are found to be ferromagnetic. Palladium is paramagnetic in the bulk but shows a very high magnetic susceptibility. It provides a huge peak in the DOS just below the Fermi energy¹ and almost fulfills the Stoner criterion for itinerant magnetism.^{2,3} As electronic devices that are based on electron spin (spintronics) benefit from a pronounced spin imbalance, tuning such materials into magnetic order is of great interest.

In systems of reduced dimension and/or coordination, appearing in small particles or clusters, wires, thin layers, and surfaces, spin ordering in Pd has been suggested theoretically⁴⁻¹² and experimentally.¹³⁻¹⁶ But also lattice defects^{1,3} or electric fields¹⁷ are considered to induce magnetism. For the case of clusters, the observed magnetism is expected to be surface related.^{13,16}

The onset of ferromagnetism in Pd is generally expected to occur at a lattice expansion of 3–7%^{1,6,18-20} with a magnetic moment of 0.12 μ_B .²⁰ Expanding volumes is experimentally difficult; however, at surfaces one has the chance to observe strong interlayer relaxations. This is for instance the case in the 1.5 ML hydrogen covered and pairing-row-reconstructed system (1 \times 2)-H/Pd(110)-pr, which shows a strong outward relaxation of the first layer calculated to be 4.4% in DFT-LDA calculations.²¹ Among the three low-index surfaces (100), (110), and (111), the (110) face is the most open one. This fact, the strong outward relaxation, and the row pairing lead to a considerably reduced coordination of the Pd atoms at the surface. Thus one should expect an enhanced tendency of the system toward magnetism. On the other hand, H adsorption usually reduces the DOS at E_F . For this reason H is generally considered to quench surface magnetism. Since surface states or resonances are sensitive to surface magnetism one may use them as a probe to detect a possible magnetic ordering.

In this paper we show that the surface resonance band at \bar{S} in clean Pd(110) is split by 400 meV in the (1 \times 2)-H/Pd(110)-pr system, very similar to the analogous surface state in magnetic Ni(110).²² In addition ARUPS measurements at 100 K show a kink structure at \sim 350 meV binding energy, which suggests

electron-magnon coupling. For further insight, first-principles density functional theory (DFT) calculations as well as spin-polarized ARUPS measurements have been performed.

The Pd(110) crystal was cut and polished to a precision of $<0.1^\circ$. It was cleaned *in situ* by cycles of Ar sputtering and annealing for 2 min at 1183 K. In order to eliminate residual carbon, this was followed by three cycles of oxygen adsorption at $T < 273$ K and subsequent flash desorption to 923 K. For preparation of the (1 \times 2)-H/Pd(110)-pr system, 0.6 L (1 L = 1×10^{-6} Torr \times 1 sec) hydrogen have been adsorbed via a leak valve at a sample temperature <170 K. Scanning tunneling microscopy (STM) measurements were performed in a variable temperature STM operated with liquid N₂. Spin-integrated ARUPS measurements were carried out with a three-channeltron analyzer at a temperature of ~ 100 K with an angular resolution of $\pm 0.7^\circ$ and an energy resolution of 50 meV. For variable-temperature photoemission an energy resolution of 70 meV was used. All presented dispersion plots are taken in constant emission angle mode. Spin-resolved ARUPS measurements were carried out at 160 K.²³ We applied magnetic field pulses of up to 200 G prior to the measurements to eventually magnetize the sample in remanence. For all photoemission experiments a photon energy of 21.2 eV from an unpolarized He lamp was used. Surface cleanliness and order were checked by low-energy electron diffraction (LEED), temperature-programmed desorption (TPD), photoemission spectroscopy, and STM. DFT calculations were carried out by means of the Vienna *ab initio* Simulation Package (VASP)²⁴ within the local density approximation (LDA).^{25,26} For the clean as well as the hydrogen-covered surface a slab of 15 layers has been calculated, with the latter being symmetrically terminated. To determine a state as a surface state or resonance, a localization of 60% in the surface layers S (S-1) and (S-2) has been chosen as a criterion.

Structural models for Pd(110) are shown in Fig. 1, together with a STM study. The clean Pd(110) system features close-packed atom rows in the topmost layer resulting in quasi-one-dimensional surface states (see description of Fig. 2). For the topmost layers an oscillatory relaxation is found with a strong inward relaxation of the first layer of $d_{1,2} = -9.5\%$ (LDA)²⁷ with respect to the bulk distance of $d_0 = 1.363$ Å. The dark

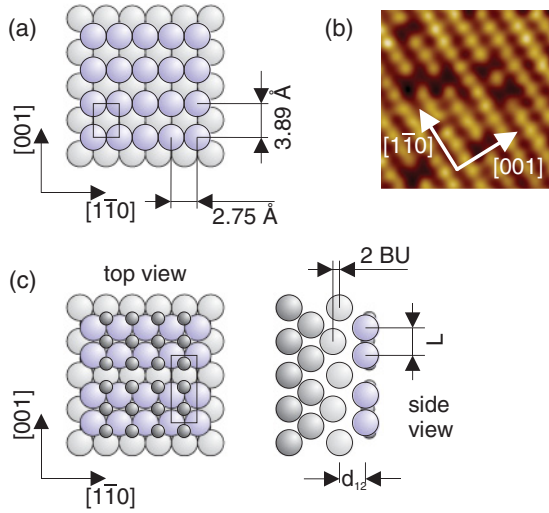


FIG. 1. (Color) Structural investigation of clean Pd(110) [(a), (b)] and the 1.5 ML hydrogen covered system (1×2) -H/Pd(110)-pr (c). The STM image is recorded at liquid N_2 temperature.

areas in Fig. 1(b) are defects resulting from the close proximity of the Pd(110) surface to the missing row reconstruction.²⁷

The adsorption of 1.5 ML hydrogen onto the clean Pd(110) surface leads to the formation of a pairing-row reconstruction. The corresponding adsorption pattern was proposed by Rieder *et al.*²⁸ based on He-scattering data and theoretically confirmed

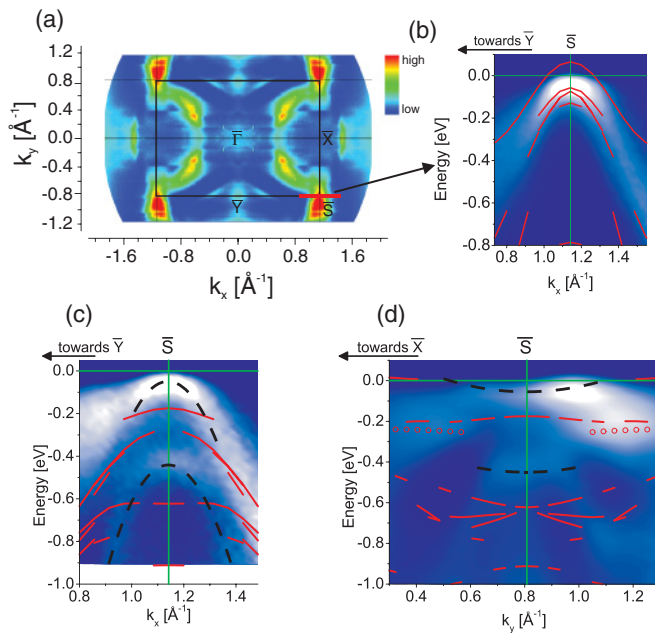


FIG. 2. (Color) (a) Fermi-surface mapping of clean Pd(110); the surface Brillouin zone (SBZ) is indicated by the black rectangle. (b) ARUPS intensity map taken along the horizontal red line in (a). (c) Same cut on the (1×2) -H/Pd(110)-pr system. (d) Cut through \bar{S} in direction $\bar{X}\bar{S}$, perpendicular to the cut in (c). To guide the eye, the dispersion of the main resonance and the satellite is indicated in (c) and (d) by the dashed line (black). Red lines and circles in (b), (c), and (d) correspond to the surface-state bands found in the LDA calculation. Color scale: Blue corresponds to low, white [red in (a)] to high photoemission intensity.

by Ledentu *et al.*²¹ The pairing-row reconstruction is accompanied by a strong buckling (BU) of 0.25 Å (LDA) in the second row and the distance between these rows is reduced by $\Delta L = -0.68$ Å (LDA).²¹ The adsorption of hydrogen reduces the amplitude of the oscillatory relaxation of the interlayer distances compared to that of the clean surface, and a strong outward relaxation of 4.4% (LDA) in $d_{1,2}$ with respect to the bulk distance d_0 is found.²¹

Details of the electronic structure of the clean and hydrogen-covered Pd(110)-surface are shown in Fig. 2. As in Pt(110),²⁹ the dominating spectral feature on the Fermi-surface map [Fig. 2(a)] is a d -derived surface resonance around \bar{S} . The energy vs. momentum cut in Fig. 2(b) shows its holelike dispersion in the $\bar{Y}\bar{S}$ direction which compares favorably to the surface-localized bands found by our LDA calculation (red lines). Similar to Pt(110) the dispersion along $\bar{X}\bar{S}$ (not shown) is roughly a factor of ~ 15 smaller than along $\bar{Y}\bar{S}$, reflecting the high anisotropy of this quasi-one-dimensional electronic state. Upon hydrogen adsorption [Figs. 2(c) and 2(d)], the surface resonance shifts only slightly toward higher binding energy. The most interesting observation is the development of a satellite peak at lower binding energy ($\Delta E = -400$ meV), which disperses parallel to the main resonance. This satellite is only found in the area around the \bar{S} surface resonance and only for coverages above 1.5 ML, where the pairing-row reconstruction is present. At lower hydrogen coverages, only the small downshift of the main resonance is observed, but no satellite. Note that the position of the surface resonance is well captured in our LDA calculations for the clean surface. For the (1×2) -H/Pd(110)-pr surface the LDA calculations predict a considerable downshift of the surface resonance as is generally expected.²¹ In the experimental data, however, we observe a strong splitting instead of a downshift. Neither the energetic positions nor the dispersion agrees with the theoretically predicted surface bands for the nonmagnetic surface.

In the following, we discuss five possible explanations for the appearance of the parallel band. (i) For the case in which the satellite is due to additional collective excitations, the 400 meV loss⁴⁴ could only stem from acoustic bulk plasmons predicted recently in Pd³⁰ or more generally from plasmons in lower dimensions^{31,32} or magnons.³³ All of these excitations, however, have “acoustic” dispersion relations starting with zero energy for zero wave vector which would not lead to a well-defined parallel satellite band. The density of states of these excitations would rather induce kinks in the band dispersion or a “peak-dip-hump” shape in the spectra (see below).

(ii) An umklapp or a backfolding of states from the \bar{X} point, being equivalent to \bar{S} in the surface Brillouin zone (SBZ) of the reconstructed (1×2) surface, might appear accidentally as a parallel dispersing band. This possibility has been ruled out by performing ARUPS measurements in the area around the \bar{X} point, which showed no corresponding intensity. Furthermore, also the LDA calculation of the clean surface does not show states at \bar{X} with appropriate energy and dispersion.

(iii) The splitting might be induced directly by hybridization of the surface resonance with hydrogen electronic states, since, e.g., the fourfold adsorption site between the paired rows (see Fig. 1) is distinguishing the pairing-row geometry from others. (iv) The surface resonance is also influenced by the

pairing-row reconstruction additionally hybridizing the states on neighboring rows. This “bonding-antibonding” splitting due to cases (iii) and (iv) should be well accounted for by the LDA calculation of the H-covered pairing-row surface. We can rule out (iii), since a charge decomposition of the calculated surface states reveals negligible hydrogen contributions. This is consistent with the absence of a significant H-induced shift of the main \bar{S} surface feature at E_F . While the calculation indeed shows the appearance of additional surface resonances around 630 meV due to the new geometry, neither the energetic position nor the dispersion relation [see Fig. 2(c)] is correctly represented in the calculations. This failure of the LDA calculation is remarkable, since for the clean surface theory and experiment agree quite precisely. Moreover, a pairing-row-related surface state in the bulk projected gap at ~ 230 meV binding energy on the H-saturated surface [circles in Fig. 2(d)] is perfectly well reproduced in the calculation and its binding energy agrees within experimental accuracy with the ARUPS spectra. Thus, it appears that for the explanation of the satellite at 400 meV effects beyond the level of LDA band calculations should be taken into account.

(v) As mentioned in the introduction, the low dimensionality of the surface system may amplify the susceptibility beyond that of Pd bulk, which raises the possibility of, e.g., a magnetic order on the surface. This is in line with Ni(110), where an enhancement of the surface magnetic moment of 13% with respect to the bulk is calculated,³⁴ and with the observed magnetic ordering at the Rh(100) surface.³⁵ For Ni(110), both clean and hydrogen-covered surfaces are magnetic and show a double-peak structure at \bar{S} .^{22,36} The splitting we find is in the range typical for exchange in d bands (170–330 meV³⁷). In order to verify such an assignment, DFT calculations including spin polarization have been carried out, but did not lead to conclusive results: Within LDA we always find a paramagnetic ground state for Pd bulk and surface, whereas using the generalized gradient approximation (GGA)³⁸ always gives a ferromagnetic splitting of ~ 300 meV at the surface as well as in the bulk. In a further attempt to probe a possible magnetic order, spin-resolved ARUPS data have been collected at 160 K. No spin polarization of the split states was found. This excludes ferromagnetic long-range order at 160 K, but does not eliminate short-range ferromagnetic domains as the source of the band splitting.

In comparison with transition temperatures of other low-dimensional magnetic systems on surfaces [e.g., $T = 15$ K for Co/Pt(997)³⁹], it is actually to be expected that the surface shows only short-range spin ordering, fluctuations, or paramagnons at higher temperatures. As paramagnons with energies up to 128 meV have been found recently in bulk Pd at temperatures between 20 and 300 K,⁴⁰ we searched for evidence of these excitations by taking ARUPS spectra at different temperatures.

In Fig. 3 we present ARUPS dispersion plots around the \bar{S} position ($k_x = 1.142 \text{ \AA}^{-1}$) recorded at 100 K. As the data were taken at constant emission angle, they have been fitted by a sum of two Lorentzian functions on a background, cutoff by the Fermi-Dirac distribution and convoluted with the experimental resolution. Black squares in Figs. 3(a) and 3(b) correspond to the energetic position of the Lorentzian. In contrast to the clean Pd(110) surface, the hydrogen-covered surface shows a

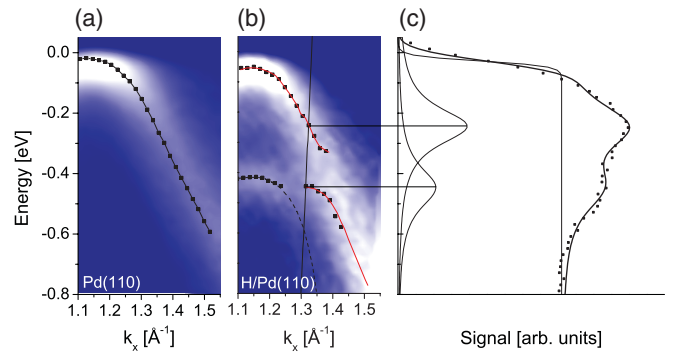


FIG. 3. (Color) ARUPS dispersion plots taken at 100 K around \bar{S} ($k_x = 1.142 \text{ \AA}^{-1}$). The direction of scanning is toward \bar{Y} . The dispersion is fitted and compared to the clean and the (1 \times 2)-H/Pd(110)-pr surface [black squares in (a) and (b), respectively]. For the hydrogen-covered system a double-peak structure can be identified (c), which is indicative of electron-magnon coupling. This is not the case for clean Pd. White corresponds to high, blue to low photoemission intensity.

clear double-peak structure around $k_x = 1.35 \text{ \AA}^{-1}$, which is explicitly shown in Fig. 3(c). The thin red lines in Fig. 3(b) are to guide the eye and show the typical behavior of electron-boson coupling.^{41,45} The interaction region is at an energetic position of ~ 350 meV binding energy.

The temperature dependence of the \bar{S} surface resonance is shown in Fig. 4. The raw data presented in Fig. 4(a) have been fitted as described above and the results are presented in Figs. 4(b) and 4(c). Considering the peak position as a function of temperature, one observes that both peaks start to move at a similar temperature with opposite direction. The total peak splitting is shown in Fig. 4(c). It is tempting to interpret it in terms of a critical behavior $\Delta E \propto (T_C - T)^\beta$ [red line

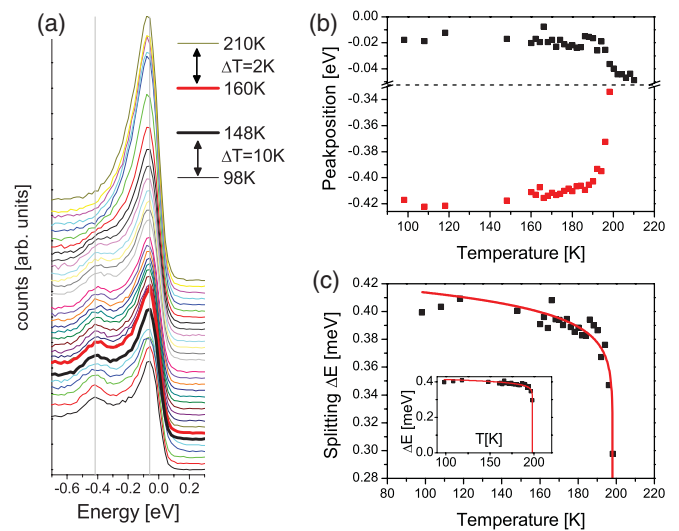


FIG. 4. (Color) Temperature-dependent evolution of spectra taken at \bar{S} . In (a) the raw data of the ARUPS measurements are shown. (b) and (c) show the temperature dependence of the peak position and distance ΔE between the peaks, as determined by fitting the data of (a). The splitting in (c) shows a critical behavior indicating a phase transition (see text).

in Fig. 4(c)]. However, the transition occurs right about the onset of H loss from the surface either through desorption or diffusion to subsurface sites, which also indicates structural changes, i.e., lifting of the (1×2) -pr reconstruction or missing and added row formation in this temperature range.^{42,43} In fact, the transition is not reversible, if the temperature is ramped up to 200 K and lowered again. Upon complete desorption of H, the main resonance shifts upward to its original position again [Fig. 2(b)].

Between 1 and 1.5 ML coverage a mixture of (1×2) -pr and (2×1) -zigzag (stable structure for 1 ML) patches is observed.⁴³ In a bonding-antibonding scenario as outlined in (iii) and (iv) above, one would generally expect a temperature-induced change in the intensity ratio of the peaks, but not a peak shift as observed in Fig. 4. This T -induced peak shift together with the other observations mentioned above seems to indicate that the splitting of the \bar{S} resonance for the (1×2) -H/Pd(110)-pr surface is caused by (short-range) ferromagnetic order. This is in contrast to conventional wisdom, which considers H to suppress surface magnetism. Generally the H $1s$ orbital hybridizes strongly with surface-state bands increasing their spatial extension and consequently their dispersion. This results normally in a reduced DOS at E_F , which is detrimental for magnetic ordering. The present case, however, is exceptional in that the \bar{S} resonance is apparently decoupled from the H $1s$ orbital. Both binding energy and dispersion remain virtually

unchanged upon H adsorption. The H decouples the surface layer from the bulk and a further dimensional reduction is brought about by the row pairing. This results in an increase of exchange and correlation which appears sufficient to induce ferromagnetic order in the surface, leading to a splitting of the \bar{S} resonance.

In conclusion we have shown that the Pd(110) system provides a peculiar peak splitting of surface resonances upon hydrogen adsorption at low temperatures. Discussing possible origins for the satellite, we have ruled out backfolding processes originating from the (1×2) -reconstruction, phonon, and plasmon excitations. As our LDA calculation is accurate for the clean surface and some of the hydrogen-induced surface states, but fails to describe the satellite, this split-off state appears not to be related to hybridizational changes upon hydrogen adsorption. The temperature shift of the peaks as well as the observation of a kink in the dispersion provide circumstantial evidence for a hydrogen-induced magnetic ordering on the surface of Pd(110). Within this magnetic interpretation, however, the lack of spin polarization in spin-resolved photoemission at 160 K indicates that the surface is in a superparamagnetic state at this temperature.

The work was supported by the Austrian Science Fund through NFN S9004 NSOS and by the University of Innsbruck through the research platform Advanced Materials.

*Now at Vorarlberg University of Applied Sciences, Hochschulstrasse 1, 6850 Dornbirn, Austria.

¹S. S. Alexandre, E. Anglada, J. M. Soler, and F. Yndurain, *Phys. Rev. B* **74**, 054405 (2006).

²J. F. Janak, *Phys. Rev. B* **16**, 255 (1977).

³N. Takano, T. Kai, K. Shiiki, and F. Terasaki, *Solid State Commun.* **97**, 153 (1996).

⁴V. Kumar and Y. Kawazoe, *Phys. Rev. B* **66**, 144413 (2002).

⁵V. Kumar and Y. Kawazoe, *Eur. Phys. J. D* **24**, 81 (2003).

⁶C. Barreteau, R. Guirado-López, D. Spanjaard, M. C. Desjonquères, and A. M. Oleś, *Phys. Rev. B* **61**, 7781 (2000).

⁷A. Delin and E. Tosatti, *J. Phys. Condens. Matter* **16**, 8061 (2004).

⁸A. Delin, E. Tosatti, and R. A. Weht, *Phys. Rev. Lett.* **92**, 057201 (2004).

⁹D. A. Stewart, *J. Appl. Phys.* **101**, 09D503 (2007).

¹⁰S. C. Hong, J. I. Lee, and R. Wu, *Phys. Rev. B* **75**, 172402 (2007).

¹¹S. C. Hong, J. I. Lee, and R. Wu, *J. Magn. Magn. Mater.* **310**, 2262 (2007).

¹²M. J. Zhu, D. M. Bylander, and L. Kleinman, *Phys. Rev. B* **42**, 2874 (1990).

¹³T. Shinohara, T. Sato, and T. Taniyama, *Phys. Rev. Lett.* **91**, 197201 (2003).

¹⁴B. Sampedro, P. Crespo, A. Hernando, R. Litrán, J. C. Sánchez López, C. López Cartes, A. Fernandez, J. Ramirez, J. González Calbet, and M. Vallet, *Phys. Rev. Lett.* **91**, 237203 (2003).

¹⁵T. Okamoto, H. Maki, Y. Oba, S. Yabuuchi, T. Sato, and E. Ohta, *J. Appl. Phys.* **106**, 023908 (2009).

¹⁶T. Taniyama, E. Ohta, and T. Sato, *Europhys. Lett.* **38**, 195 (1997).

¹⁷Y. Sun, J. D. Burton, and E. Y. Tsymbal, *Phys. Rev. B* **81**, 064413 (2010).

¹⁸H. Chen, N. E. Brener, and J. Callaway, *Phys. Rev. B* **40**, 1443 (1989).

¹⁹L. Fritsche, J. Noffke, and H. Eckhardt, *J. Phys. F* **17**, 943 (1987).

²⁰V. L. Moruzzi and P. M. Marcus, *Phys. Rev. B* **39**, 471 (1989).

²¹V. Ledentu, W. Dong, P. Sautet, G. Kresse, and J. Hafner, *Phys. Rev. B* **57**, 12482 (1998).

²²W. Eberhardt, E. W. Plummer, K. Horn, and J. Erskine, *Phys. Rev. Lett.* **45**, 273 (1980).

²³M. Budke, T. Allmers, M. Donath, and G. Rangelov, *Rev. Sci. Instrum.* **78**, 113909 (2007).

²⁴G. Kresse and J. Furthmüller, *Phys. Rev. B* **54**, 11169 (1996).

²⁵J. P. Perdew and A. Zunger, *Phys. Rev. B* **23**, 5048 (1981).

²⁶D. M. Ceperley and B. J. Alder, *Phys. Rev. Lett.* **45**, 566 (1980).

²⁷C. Franchini, Ph.D. thesis, Univ. Vienna, 2002.

²⁸K. H. Rieder, M. Baumberger, and W. Stocker, *Phys. Rev. Lett.* **51**, 1799 (1983).

²⁹M. Minca, S. Penner, E. Dona, A. Menzel, E. Bertel, V. Brouet, and J. Redinger, *New J. Phys.* **9**, 386 (2007).

³⁰V. M. Silkin, I. P. Chernov, Y. M. Koroteev, and E. V. Chulkov, *Phys. Rev. B* **80**, 245114 (2009).

³¹M. Rocca, *Surf. Sci. Rep.* **22**, 1 (1995).

³²J. M. Pitarke, V. M. Silkin, E. V. Chulkov, and P. M. Echenique, *Rep. Prog. Phys.* **70**, 1 (2007).

³³A. Hofmann, X. Y. Cui, J. Schäfer, S. Meyer, P. Höpfner, C. Blumenstein, M. Paul, L. Patthey, E. Rotenberg, J. Bünemann *et al.*, *Phys. Rev. Lett.* **102**, 187204 (2009).

³⁴H. Krakauer, A. J. Freeman, and E. Wimmer, *Phys. Rev. B* **28**, 610 (1983).

- ³⁵A. Goldoni, A. Baraldi, G. Comelli, S. Lizzit, and G. Paolucci, *Phys. Rev. Lett.* **82**, 3156 (1999).
- ³⁶E. Boschung, T. Pillo, J. Hayoz, L. Patthey, P. Aebi, and L. Schlapbach, *J. Electron Spectrosc. Relat. Phenom.* **101–103**, 349 (1999).
- ³⁷T. J. Kreuz, T. Greber, P. Aebi, and J. Osterwalder, *Phys. Rev. B* **58**, 1300 (1998).
- ³⁸J. P. Perdew, K. Burke, and M. Ernzerhof, *Phys. Rev. Lett.* **77**, 3865 (1996).
- ³⁹P. Gambardella, *J. Phys. Condens. Matter* **15**, S2533 (2003).
- ⁴⁰R. Double, S. M. Hayden, P. Dai, H. A. Mook, J. R. Thompson, and C. D. Frost, *Phys. Rev. Lett.* **105**, 027207 (2010).
- ⁴¹S. Hüfner, editor, *Very High Resolution Photoelectron Spectroscopy* (Springer, Berlin, 2007).
- ⁴²J.-W. He, D. Harrington, K. Griffiths, and P. Norton, *Surf. Sci.* **198**, 413 (1988).
- ⁴³J. Yoshinobu, H. Tanaka, and M. Kawai, *Phys. Rev. B* **51**, 4529 (1995).
- ⁴⁴A strong-coupling scenario allowing multiboson excitations can be excluded as the strong dispersion along the chain indicates delocalized photoholes.
- ⁴⁵Depending on the direction of fitting (at constant energy or momentum, respectively) the appearance of the fitted peak maximum varies.